BRAGE IMR

Brage IMR –

Havforskningsinstituttets institusjonelle arkiv

Dette er forfatters siste versjon av den fagfellevurderte artikkelen, vanligvis omtalt som postprint. I Brage IMR er denne artikkelen ikke publisert med forlagets layout fordi forlaget ikke tillater dette. Du finner lenke til forlagets versjon i Brage-posten.
Det anbefales at referanser til artikkelen hentes fra forlagets side.

Ved lenking til artikkelen skal det lenkes til post i Brage IMR, ikke direkte til pdf-fil.

Brage IMR –

Institutional repository of the Institute of Marine Research

This is the author's last version of the article after peer review and is not the publisher's version, usually referred to as postprint. You will find a link to the publisher's version in Brage IMR. It is recommended that you obtain the references from the publisher's site.

Linking to the article should be to the Brage-record, not directly to the pdf-file.

HAVFORSKNINGSINSTITUTTET
INSTITUTE OF MARINE RESEARCH

Foto: Leif Nøttestad

This is a pre-copy-editing, author-produced PDF of an article accepted for publication in ICES Journal of Marine Science following peer review. The definitive publisher-authenticated version of Pedersen, G., Handegard, N. O., and Ona, E. 2009. Lateral-aspect, target-strength measurements of in situ herring (Clupea harengus). – ICES Journal of Marine Science, 66: 1191–1196 is available online at: http://icesjms.oxfordjournals.org/content/66/6/1191

Lateral-aspect target strength measurements of *in situ* herring (*Clupea harengus*)

Geir Pedersen, Nils Olav Handegard, Egil Ona

Pedersen, G., Handegard, N.O., Ona, E., 2009. Lateral-aspect target strength measurements of *in situ* herring (*Clupea harengus*). – ICES Journal of Marine Science, 66: 000-000.

Surveys of schooling herring with the new multi-beam sonar (Simrad MS70) pose new challenges when converting the echo energy to estimates of biomass. Since the sonar projects horizontally, data and models of lateral-aspect herring target strength *TS* are needed. In this study, *TS* of herring are measured with a horizontally-projecting split-beam echosounder (Simrad EK60). Target tracking methods are used to estimate swimming angles relative to the horizontal θ of individual herring within schools and layers, and to evaluate how θ and *TS* change vs. depth *z*. Measurements of θ and *TS* are input to a model describing *TS* as a function of θ and *z*. The results indicate that the mean lateral-aspect *TS* of *in situ* herring depends on *z*. Moreover, the mean lateral-aspect *TS* is more sensitive to *z* than is the mean dorsal-aspect *TS* predicted by a published model. At z = 50 m, the mean lateral-aspect *TS* is nearly 2.5 dB higher than the mean dorsal-aspect *TS*. Conversely, at z = 350 m, the lateral-aspect *TS* is 5 dB lower. These results suggest that herring swimbladders do not compress uniformly with increasing pressure, but compress dorso-ventrally more than laterally.

Keywords: acoustics, target strength, *in situ*, split-beam, herring, depth dependence.

Running Heads: Lateral-aspect *TS* of herring – G. Pedersen *et al.*

Received 8 August 2009; accepted .

Geir Pedersen, Nils Olav Handegard, Egil Ona: Institute of Marine Research, PO Box 1870, 5817 Bergen, Norway. Correspondence to Geir Pedersen: tel: +47 55 23 85 00; fax: +47 55 23 85 84; e-mail; geir.pedersen@imr.no

Introduction

Scientific echosounders are routinely utilized for estimating abundances of fish stocks and for mapping their spatial and temporal distributions. To obtain accurate acoustic estimates of fish abundance, accurate mean target strength (*TS*) is needed. This paper presents *TS* obtained from lateral-aspect measurements of *in situ* Norwegian spring spawning herring (*Clupea harengus* L.). In freshwater, rivers in particular, the lateral-aspect *TS* is important for acoustic surveys of fish (Kubecka, 1994; Lilja *et al*., 2000; 2004, Frouzová *et al*., 2005). With increased use of calibrated multibeam sonars (Andersen *et al*., 2006) for herring abundance estimation, their lateral-aspect *TS* will become increasingly important. The MS70 multibeam sonar was developed by Simrad Norge AS, in collaboration with the Norwegian Institute of Marine Research and the French Research Institute for Exploitation of the Sea, and installed on the RV "G. O. Sars" for the specific purpose of measuring herring schools.

The same principles apply for measurements of lateral- and dorsal-aspect *TS* (Simmonds and MacLennan, 2005); however, larger variations in lateral-aspect *TS* occur as the fish can be insonified over a potentially uniform distribution of yaw, i.e. incidence angles ranging from head to tail (Kubecka, 1994; Lilja *et al*., 2000, 2004; Frouzová *et al.*, 2005). *TS* measurements of anaesthetized or immobilized fish were made vs. incidence angles ranging from 0-360° in the horizontal plane (Love, 1969; 1977; Haslett, 1977). These measurements showed a very strong backscattering directivity pattern with a maximum *TS* near side aspect and low *TS* in the tail and head aspects. The mean side-aspect *TS* is therefore expected to be an average over a uniform distribution of yaw angle.

The Norwegian spring-spawning herring is an important stock in the Northeast Atlantic ecosystem (Dragesund *et al.*, 1980). The spawning stock for 2006 was estimated to be near 10.3 million tons, with a management strategy implying a maximum catch of 1.28 million tons in 2007 (ICES, 2006). Many researchers have estimated *TS* of *in situ* and *ex situ* herring (e.g. Foote *et al*., 1986; Rudstam *et al*., 1988; Kautsky *et al*., 1990; Reynisson, 1993; Huse and Ona, 1996; Ona, 2003; Didrikas and Hansson, 2004; Peltonen and Balk, 2005). The mean *TS* vs. log-length relationship currently used in acoustic biomass assessment of Norwegian spring spawning herring at 38 kHz is based on the recommendations by Foote (1987), $TS = 20\log(L) - 71.9$, where L is the fish length (cm). The assessment of this stock is based on results from acoustic surveys in several areas including the over-wintering area. Because herring form very dense aggregations, it is difficult to obtain good *TS* measurements of *in situ* individuals.

Advances in pressure-stabilized transducers during the last decade provide new possibilities to submerge transducers within schools and dense layers and make calibrated *TS* measurements. Until now, the average *TS* of Norwegian spring spawning herring was explored experimentally (Ona, 2003) and theoretically (Gorska and Ona, 2003a and b; Fässler *et al*., 2008), showing that the mean dorsal-aspect *TS* is clearly dependent on depth. Ona (2003) presented a mean *TS* vs. log-length relationship for Norwegian spring spawning herring at 38 kHz, which includes a parameter for the effect of depth (z): $TS = 20\log(L) - 2.3\log(1+z/10) - 65.4$. Ona also showed that the backscattering directivity of herring is similar at all depths, which indicates that the length of the swimbladder is stable. The factor 2.3 in Ona's equation is consistent with a dorsal-ventral compression, rather than a uniform compression. Herring, which are physostomes, are probably unable to secrete gas into the swimbladder (Brawn, 1969; Blaxter and Batty, 1984; Ona, 1984; 1990), so its volume probably decreases with increasing depth. Since the swimbladder accounts for 90-95 % of the backscattered acoustic signal at 38 kHz (Foote, 1980), the backscattering cross-section σ_{bs} of herring should decrease with increasing pressure. Exactly how σ_{bs} decreases with z is largely determined by the shape of the swimbladder, and how this changes during compression.

The objectives of the paper are to estimate the mean lateral-aspect *TS* of *in situ* herring and characterize its dependence on pressure. The latter may suggest how the herring swimbladder is compressed and how its volume changes vs. pressure.

Methods

Measurements of lateral-aspect *TS* were made during the yearly mapping of the Norwegian spring spawning herring stock in the Ofotfjord/Vestford wintering area in December 2001 and January 2002. The stock was distributed throughout the Ofotfjord in very dense layers, requiring the transducer to be lowered into the layer to resolve individual fish. Therefore, all measurements were restricted to short ranges (<30 m).

Lateral-aspect *TS* data were recorded from RV "Johan Hjort" using a submerged transducer (Simrad 38DD) connected to a split-beam echosounder (Simrad EK60). The research vessel was maintained at a fixed position before each experiment and all onboard lighting and acoustic instrumentation were powered off. The transducer was aimed horizontally and lowered into the dense herring layers. A vane mounted on the top of the transducer ensured that it pointed directly into the weak fjord current. The transducer was held at a constant depth within the herring layer during each measurement series. The method is discussed in more detail in Ona (2003), where in the same transducer was deployed but aiming vertically downwards.

A total of 24 experiments were conducted on herring with a typical vertical distribution from z = 50-350 m. The experiments consisted of measurements at a fixed depth, typically lasting 30-60 minutes. Measurements were made between ranges from 5-30 m with a pulse repetition frequency of 10-17 Hz. See Table 1 for other echosounder parameters.

The echosounder system was calibrated before and after *TS* measurements using the standard sphere method (Foote *et al*., 1987) and Simrad calibration software. The transducer was orientated vertically. Measurements of water temperature, salinity, density and sound speed were measured with a CTD (Sea-Bird SBE9, Sea-Bird Electronics Inc., Bellevue, USA). The standard target was a 60 mm diameter copper sphere with *TS* at 38 kHz = -33.6 dB re $1m^2$ for sound speed equal to 1490 m/s. The sphere was moved through the acoustic beam at 10 m range using three motorized winches attached to the rails of the ship.

Although the transducer is pressure stabilised, its performance does change with depth. Therefore, a second calibration characterized the performance of the system vs. depth. The sphere was positioned under the transducer at a distance of 6.21 m from the active transducer face. The transducer and sphere were lowered from the surface in several steps down to z = 400 m and then raised in several steps to the surface. This procedure investigated potential hysteresis effects. Potential variation in the sphere *TS* was evaluated relative to the local environmental conditions (i.e. the densities and sound speeds of the sphere and the seawater) The results from this calibration were used to compensate the measured *TS* with depth.

Many single echo detection (SED) algorithms are available to reject backscatter from multiple unresolved targets (see e.g. Soule *et al*., 1995 for an evaluation of conventional methods). Instead of relying on the SED algorithm in the EK60, which does not consider the temporal evolution of successive signals. The split-beam data in .raw format were processed in Matlab (The Mathworks, USA) using algorithms described in Handegard (2007) to extract tracks of individual fish. Each echogram pixel has a spatial position defined by measurements of range (r) and two split-beam angles (α, β), and this is mapped to Cartesian coordinates (e.g. Handegard *et al*., 2005, Appendix B).The "track-before-detect" method uses coherence in the positions of each pixel > -70 dB to identify the fish tracks. Several metrics including: phase deviation within a track; mismatch between forward- and backward-track positions; and proximity to other tracks are combined to estimate the quality of each track (Handegard 2007, his Equation (12)). The tracking parameters used in this analysis are the same as for data set I in Handegard (2007, his Table II). The positions and mean apparent velocity along a track are estimated by a linear regression through the target positions with time. For each track, the target strength (*TS*) is estimated for each ping by applying time varied gain and beam-pattern corrections (Myriax, 2008). Each observation dataset includes estimates of the positions of the target in the beam, its mean velocity for the track, and the *TS* for each detection within a track.

The vane on the transducer aligns the acoustic axis with the water current. The water current is estimated by a 100-point running-mean filter (nearly seven seconds) on the mean along-axis component of the apparent track velocity. The estimated water current estimate is subtracted from the apparent track velocity, resulting in an estimated swimming velocity. Ignoring the depth component *z* of the track position, the angle of the track relative to the acoustic axis is estimated by:

$$\theta = \cos^{-1}\left(\frac{\boldsymbol{x}\cdot\boldsymbol{v}}{|\boldsymbol{x}||\boldsymbol{v}|}\right), \quad (1)$$

where $\boldsymbol{x}$ is the *x*-*y*-position and $\boldsymbol{v}$ is the estimated swimming velocity projected onto the horizontal plane. The $\theta = 0°$ and 180°for tracks moving away and towards the transducer, respectively. The resulting sets of *TS*, θ and *z*. were filtered with respect to *TS* > -60 dB, α and $\beta < \pm 4.0°$, and track quality = 3.5 (see Handegard, 2007).

The tracked targets were sampled after each experiment using a 16x16 fathom capelin trawl ("Harstad" trawl). The trawl was equipped with a multi-sampler (Engås *et al*., 1997) to obtain discrete samples at different depths. The performance of the trawl was monitored using trawl-mounted instrumentation (SCANMAR AS, Norway). Length and other biological parameters were measured for all captured fish.

Model

Boyle-Mariotte's law states that, at constant temperature, the absolute pressure and volume of a gas are inversely proportional. Therefore, the volume *V* of a fish swimbladder at *z*, can be related to its volume at the surface V_0

$$V(z)=V_0(1+z/10)^{\gamma}, \quad (2)$$

Where γ is a dimensionless depth-compression factor. To estimate γ, the measurement of *TS*, θ and *z* were fit to the following equation using the method of least-squares:

$$TS(\theta, z) = TS_0(\theta) + 10\gamma \log\left(1+\frac{z}{10}\right). \quad (3)$$

TS_0 is the *TS* at the surface; it was estimated by as the mean TS_0 in 5° bins of θ and various bins of *z* (see Figures 1 and 2).

Results

The lengths of Norwegian spring spawning herring caught in trawls associated with the *TS* measurements were *L* = 32.1 cm (s.d. = 2.0 cm). In addition to herring, some saithe (*Pollachius virens* L.), cod (*Gadus morhua* L.), and blue whiting (*Micromesistius poutassou* L.) were caught. The analyzed acoustic measurements correspond to trawl catches of > 95 % herring by number. There was no significant correlation between *z* and *L* of herring captured in the same depth (r^2=0.0974; $p < 0.05$).

The calibration of the transducer vs. depth showed measurements of the sphere *TS* were 0.1-0.2 dB higher than the nominal value of –33.6 between depths of 25 and 50 m, and 1 dB lower near 150-200 m. At greater depths, the measured *TS* increased approaching the nominal value. These results were used to compensate the *TS* for system gain vs. transducer depth.

Estimates of γ and $TS_0(\theta)$ depend on the selected thresholds on α, β, and track quality (Table 2). The mean *TS* in 5° bins of θ are plotted vs. 1 m bins of *z* (Figure 1). All of the curves peak at $\theta > 90°$, particularly for large *z*. For $\theta < 90°$, fewer measurements results in a larger variance.

Apparently, more fish swim at $\theta > 90°$ (Figure 2a). The majority of the fish swam with or perpendicular to the current in the fjord. At depths between 50-100 m, the largest number of detections was in the 100° bin. At depths between 200-350 m, the maximum single target detections were at $\theta > 90°$. There were more single target detections between 50-100 m than between 200-350 m (Figure 2a).

Within each $\theta = 5°$ bin, the average number of single target detections was 3321. Ona (2003) estimated that for 500-1000 estimates, the s.e. of σ_{bs} is < 5 % of the mean. In these experiments, for large z and small θ, fewer measurements resulted in a larger s.e. (Figures 2a and b). However, increasing the bin size from $\theta = 5°$to 10° did not change the estimated TS_0, although the estimated γ changed by 2.5 %.

The least sum-of-squares in equation (3) yielded γ = -1.2. This value was used to calculate $TS_0(\theta)$; $TS_0(90°)$ = -25.0 dB. Equation (3) also predicts TS (z); TS(50 m) = -34.5 dB and TS(100 m) = -37.2 dB. All of the TS curves are shown in Figure 2b, along with the best fit estimate of $TS_0(\theta)$. Residuals (i.e. the difference between the best fit and the $TS_0(\theta)$ curves) for all depths are shown in Figure 2c. In Figure 2d the resulting depth dependent lateral-aspect TS model is plotted with a dorsal aspect model (Ona, 2003).

Discussion

The distribution of θ was not uniform with z, and the measurements at $z > 200$ m differed from those at smaller z. At $z > 100$ m, most fish appeared to swim against the current in the fjords. There is a higher variation in $TS(\theta)$ for the shallower measurements. The maximum lateral-aspect TS generally occurs at near normal incidence (e.g. Love, 1969; 1977). In these experiments, the TS averaged over $\theta = 5°$ bins did not show a clear peak for depths greater than 200 m.

The estimation of θ depends on estimates of $\boldsymbol{x}$ and $\boldsymbol{v}$. The process of estimating tracks from pixels may overestimate $\boldsymbol{v}$ which can affect the estimates of θ. Estimating $\boldsymbol{v}$ from a linear regression of positions does not account for the fish-track curvature. The estimates of water velocity assume that the transducer beam-axis was aimed into the current, and the length of the running mean filter is sufficiently long to suppress the affect of fish behaviour. However, if fish swimming speed is very polarized, this assumption is invalid.

Estimates of lateral-aspect TS appear to differ for herring swimming away vs. towards the transducer. This may be an artefact of biases in estimates of θ resulting from few detections at small θ. Perhaps some of the measurement variation results from real variation in the scattering directivity pattern of herring.

Swimming movements cause within-track variations in fish TS (Handegard *et al*., 2009). Sinusoidal variation may be filtered in estimates of mean TS, allowing the affects of swimbladder volume to be assessed. Conversely, changes in swimbladder volume and swimming behaviour may be inextricably linked. For example, swimming activity could increase with depth to compensate for negative buoyancy, which could cause convex-concave oscillations in the swimbladder and bias in mean TS vs. depth.

The measured lateral-aspect TS varied greatly vs. z. As shown in Figure 2d, the TS at z = 50 metres is 9.5 dB higher than at z = 350 meters. At a depth of 50 m, the mean lateral-aspect TS, using the estimated depth model, was -34.5 dB; for comparison, the mean dorsal-aspect TS (Ona, 2003) was -37.0 dB. At z = 95 m, the lateral- and dorsal-aspect TS are both -37.6 dB. This indicates that increased pressure causes the swimbladder height to decrease more than its width.

Equation (3) predicts a precipitous decrease in TS vs. z, implying a corresponding decreasing in swimbladder size. For a model that adheres to Boyle-Mariotte's law (i.e. $2\delta + \varepsilon = 1$), two sets of parameters have been proposed for the width contraction δ and length contraction ε of a herring's swimbladder: $\delta = 1/3$, $\varepsilon = 1/3$; and $\delta = 1/2$ and $\varepsilon = 0$ (Ona, 2003; Gorska and Ona, 2003a; 2003b). Fässler *et al*. (2008) deem the latter values to be most realistic. In any case,

backscatter at 38 kHz is sensitive to the cross-sectional area and shape of the herring swimbladder, and not its volume.

According to Blaxter (1979), the herring swimbladder is not prolate spheroid and changes in its dimensions vs. pressure will not be uniform. He measured the contraction of herring swimbladders by exposing fish to two to four atmospheres in a pressure chamber. The central vertical dimension of the swimbladder contracted more than the horizontal dimension. The regions near the ends of the swimbladder were less affected by pressure than the central region indicating that the length of the swimbladder was not appreciably affected by increases in pressure. From this he was concluded that the swimbladder flattens with increased pressure into a shallow ellipse. In contrast, the results in Figure 2d indicate that the height but also the length of the herring swimbladder are affected by changes in pressure.

The steep slope of the curve (Figure 2d) may be the result of inadvertently including larger targets like saithe.Video or photo-validation of target species would have improved the accuracy of the measurements. However, artificial lighting would have disturbed the natural behaviour of the herring. Concurrent use of a high frequency imaging sonar (e.g., DIDSON, Beltcher *et al*., 2002), may also have improved target recognitions, without the need to artificial lighting.

Currently, there are no quality MS70 measurements of lateral-aspect *TS* of *in situ* herring. Once available, they should be compared to the measurements in this study. Also, controlled measurements of *TS* of live herring vs. pressure and incidence angle are needed to understand and accurately model the effects of swimbladder compression on their three-dimensional scattering directivities.

References

Andersen, L. N., Berg, S., Gammelseter, O. B., and Lunde, E. B. 2006. New scientific multibeam systems (ME70 and MS70) for fishery research applications. Journal of the Acoustical Society of America, 120: 3017.

Engås, A., Skeide, R., and West, C. W. 1997. The «Multisampler»: a system for remotely opening and closing multiple codends on a sampling trawl. Fisheries Research, 29: 295-298.

Belcher, E., Hanot, W., and Burch, J. 2002. Dual-Frequency Identification Sonar (DIDSON). Proceedings of the 2002 International Symposium on Underwater Technology, 187-192.

Blaxter, J. H. S. 1979. The herring swimbladder as a gas reservoir for the acoustico-lateralis system. Journal of Marine Biological Society of the United Kingdom, 59: 1-10.

Blaxter, J. H. S., and Batty, R. S. 1984. The herring swimbladder: loss and gain of gas. Journal of Marine Biological Society of the United Kingdom, 64: 441-459.

Brawn, V. M. 1969. Buoyancy of Atlantic and Pacific herring. Journal of the Fisheries Board of Canada, 26: 2077-2091.

Didrikas, T., and Hansson, S. 2004. In situ target strength of the Baltic Sea herring and sprat. ICES Journal of Marine Science, 61: 378-382.

Dragesund, O., Hamre, J., and Ulltang, Ø. 1980. Biology and population dynamics of the Norwegian spring-spawning herring. Rapports et Procès-Verbaux des Réunions du Conseil International pour l'Exploration de la Mer, 177: 43-71.

Fässler, S. M. M., Gorska, N., Ona, E., and Fernandes, P. G. 2008. Differences in swimbladder volume between Baltic and Norwegian spring-spawning herring: Consequences for mean target strength. Fisheries Research, 92: 314-321.

Foote, K. G. 1987. Fish target strengths for use in echo integrator surveys. The Journal of the Acoustical Society of America, 82: 981-987.

Foote, K. G. 1980. Importance of the swimbladder in acoustic scattering by fish: a comparison of gadoid and mackerel target strengths. Journal of the Acoustical Society of America, 67: 2084-2089.

Foote, K. G., Aglen, A., and Nakken, O. 1986. Measurement of fish target strength with a split-beam echo sounder. Journal of the Acoustical Society of America, 80: 612-621.

Foote, K. G., Knudsen, H. P., Vestnes, G., Maclennan, D. N., and Simmonds, E. J. 1987. Calibration of acoustic instruments for fish density estimation: a practical guide. ICES Cooperative Research Report No. 144, 57 pp.

Frouzová, J., Kubečka, J., Balk, H., Frouz, J. 2005. Target strength of some European fish species and its dependence on fish body parameters. Fisheries Research, 75: 86–96.

Gorska, N., and Ona, E. 2003a. Modeling the acoustic effect of swimbladder compression in herring. ICES Journal of Marine Science, 60: 548-554.

Gorska, N., and Ona, E. 2003b. Modeling the effect of swimbladder compression on the acoustic backscattering from herring at normal or near-normal dorsal incidences. ICES Journal of Marine Science, 60: 1381-1391.

Handegard, N. O. 2007. Observing individual fish behavior in fish aggregations: Tracking in dense fish aggregations using a split-beam echosounder. Journal of the Acoustical Society of America, 122: 177-187.

Handegard, N. O., Patel, R., and Hjellvik, V. 2005. Tracking individual fish from a moving-platform using a split-beam transducer. Journal of the Acoustical Society of America, 118: 2210-2223.

Handegard, N. O., Pedersen, G., and Brix, O. 2009. Estimating tailbeat frequency using split-beam echosounders. ICES Journal of Marine Science, 66: 1252–1258

Haslett, R. W. G. 1977. Automatic plotting of polar diagrams of target strength of fish in roll, pitch and yaw. Rapports et Proceès-verbaux des Réunions, Conseil International pour l'Exploration de la Mer, 170: 74-91

Huse, I., and Ona, E. 1996. Tilt angle distribution and swimming speed of overwintering Norwegian spring spawning herring. ICES Journal of Marine Science, 53: 863-873.

Kautsky, G. A., Lemberg, N. A., and Ona, E. 1990. In situ target strength measurements of Pacific herring (*Clupea harengus pallasi*) in the eastern Strait of Georgia using dual-beam and split beam sonar. Proceedings of the International Herring Symposium, Oct 1990, Anchorage, Alaska. 163-182.

Kubecka, J. 1994. Simple model on the relationship between fish acoustical target strength and aspect for high-frequency sonar in shallow waters. Journal of Applied Ichthyology-Zeitschrift Fur Angewandte Ichthyologie, 10: 75-81.

ICES. 2006. Report of the Northern Pelagic and Blue Whiting Fisheries Working Group, 24-30 August 2006, ICES CM 2006/ACFM: 34.

Lilja, J., Marjomaki, T. J., Riikonen, R., and Jurvelius, J. 2000. Side- aspect target strength of Atlantic salmon (*Salmo salar*), brown trout (*Salmo trutta*), whitefish (*Coregonus lavaretus*), and pike (*Esox lucius*). Aquatic Living Resources, 13: 355-360.

Lilja, J., Marjomaki, T. J., Jurvelius, J., Rossi, T., and Heikkola, E. 2004. Simulation and experimental measurement of side- aspect target strength of Atlantic salmon (*Salmo salar*) at high frequency. Canadian Journal of Fisheries and Aquatic Sciences, 61: 2227-2236.

Love, R. H. 1977. Target strength of an individual fish at any aspect. Journal of the Acoustical Society of America, 62: 1397-1403.

Love, R. H. 1969. Maximum side-aspect target strength of an individual fish. Journal of the Acoustical Society of America, 46: 746-752.

Myriax. 2008. Help file 4.40.26 for Echoview. 4.40.63.

Ona, E. 2003. An expanded target-strength relationship for herring. ICES Journal of Marine Science, 60: 493-499.

Ona, E. 1990. Physiological factors causing natural variations in acoustic target strength of fish. Journal of the Marine Biological Association of the United Kingdom, 70: 107-27.

Ona, E. 1984. In situ observations of swimbladder compression in herring. ICES CM 1984/B: 18.

Peltonen, H., and Balk, H. 2005. The acoustic target strength of herring (*Clupea harengus* L.) in the Northern Baltic Sea. ICES Journal of Marine Science, 624: 803-808.

Reynisson, P. 1993. In situ target strength measurements of Icelandic summer-spawning herring in the period 1985-1992. ICES CM 1993/B: 40.

Rudstam, L., Lindem, T., and Hansson, S. 1988. Density and in situ target strength of herring and sprat: a comparison between two methods of analyzing single beam sonar data. Fisheries Research, 6: 305-315.

Simmonds, E. J., and Maclennan, D. N. 2005. Fisheries Acoustics: Theory and Practice, Blackwell Publishing.

Soule, M., Barange, M., and Hampton, I. 1995. Evidence of bias in estimated abundance of target strength obtained with a split beam echo-sounder. ICES Journal of Marine Science, 52: 139-144.

Tables

Table 1. Instrument technical specifications and parameter settings used for herring *TS* measurements.

Simrad EK60 – 38 kHz	Value	Units
Transducer Type	ES38DD	-
Absorption coefficient	10	dB km^{-1}
Pulse duration	0.512	ms
Bandwidth	3.28	kHz
Transmitting power	200	W
Two-way beam angle	-20.6	dB
Alongship angle sensitivity	21.9	deg
Athwartship angle sensitivity	21.9	deg
Transducer gain	20.7	dB
Alongship 3 dB beamwidth	6.81	deg
Athwartship 3 dB beamwidth	7.08	deg
Alongship offset angle	-0.04	deg
Athwarthsip offset angle	-0.16	deg
s_A-correction	-0.60	dB

Table 2. Estimated γ and TS_0 (Equation 3) vs. varying maximum allowed alongship (α) and athwartship (β) angles, and track-quality criterion (measure of association error in target tracking). No track-quality criterion was set when calculating γ and TS_0 for different maximum allowed angles, and no maximum allowed angle was set when calculating γ and TS_0 using different track-quality criteria.

Max. α, β	γ	TS_0	Quality	γ	TS_0
0.5	-0.0463	-38.1515	0.5	-0.0470	-35.2931
1	-1.3904	-23.9853	1	-0.0285	-34.8979
1.5	-1.3894	-23.9823	1.5	-0.0310	-35.7430
2	-1.3895	-23.9239	2	-0.0326	-36.1928
2.5	-1.3890	-23.8956	2.5	-1.1849	-25.0815
3	-1.2906	-24.6818	3	-1.0880	-26.0275
3.5	-1.2898	-24.1178	3.5	-1.0884	-26.0938
4	-1.1908	-25.4049	4	-1.0885	-26.1537
4.5	-1.1895	-25.3472	4.5	-1.0885	-26. 2184
5	-1.0905	-26.1749	5	-1.0885	-26. 2184
5.5	-1.0897	-26.1723	5.5	-1.0885	-26. 2184
6	-1.0891	-26.1887	6	-1.0885	-26. 2184
6.5	-1.0886	-26.2093	6.5	-1.0885	-26. 2184
7	-1.0885	-26.2184	7	-1.0885	-26.2184

Figure captions

Figure 1. Measured lateral-aspect *TS* of *in situ* herring averaged over 5° swimming-angle (θ) bins at each of the measurement depths (z).

Figure 2. a) the number of single-fish detections averaged over 5° swimming-angle (θ) bins; b) estimated $TS_0(\theta)$ for each measurement depth (z), and the best-fit curve (dashed line); c) residuals from a least-squares fit of Equation (5); d) depth dependency of lateral-aspect *TS* compared with a dorsal-aspect *TS* model with γ = -0.23 and TS_0 = -35.3 dB (Ona, 2003).

Figure 1.

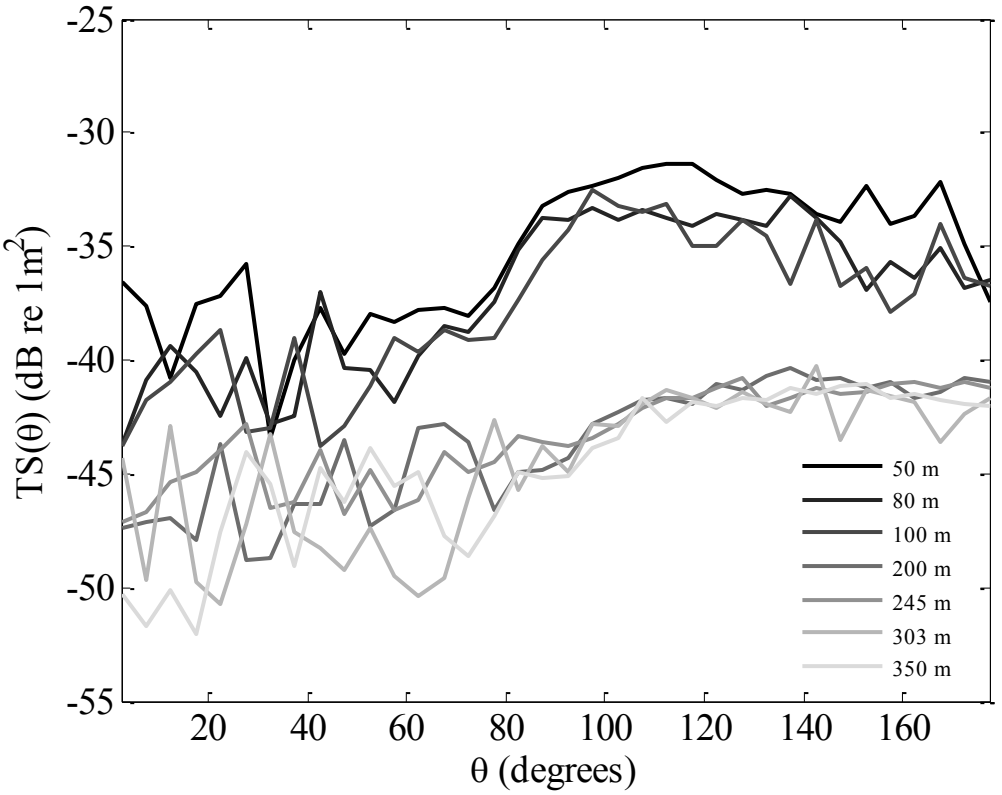
-25
-30
-35
-40
-45
-50
-55
TS(θ) (dB re 1m²)
20
40
60
80
100
120
140
160
θ (degrees)
50 m
80 m
100 m
200 m
245 m
303 m
350 m

Figure 2.

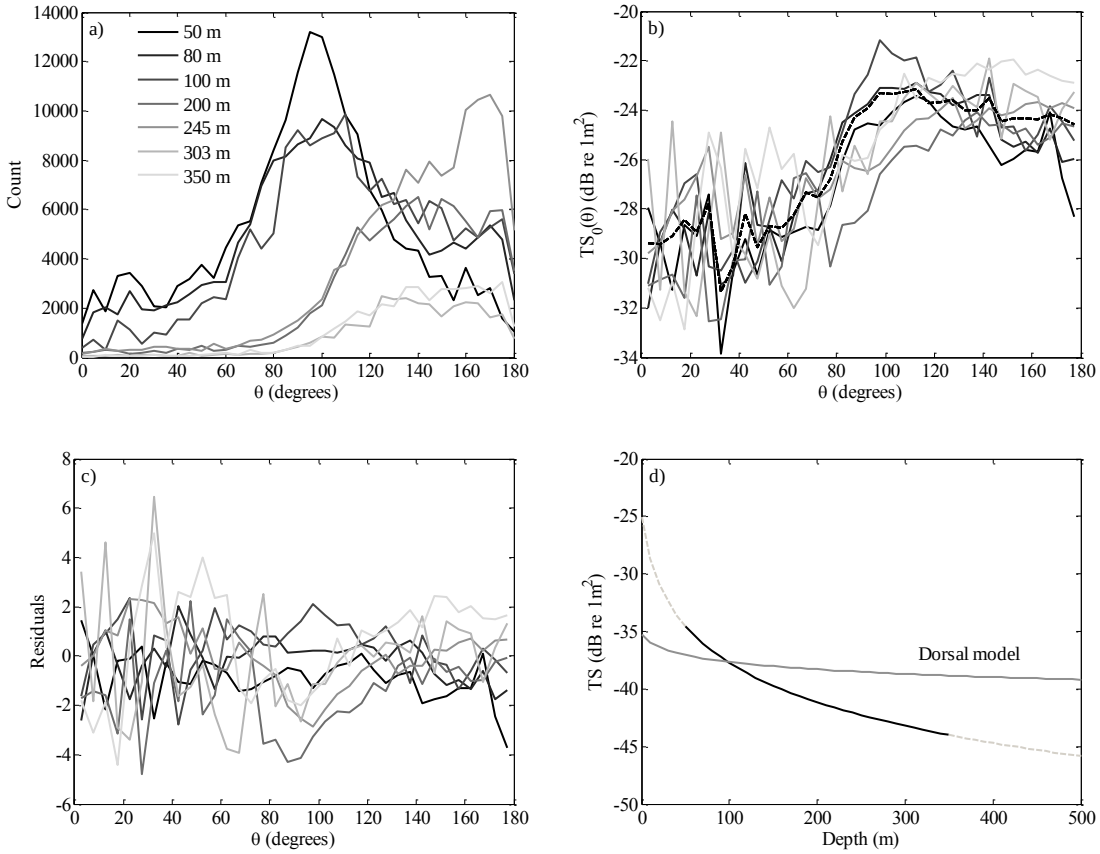
a)
50 m
80 m
100 m
200 m
245 m
303 m
350 m
Count
θ (degrees)
b)
TS0(θ) (dB re 1m2)
θ (degrees)
c)
Residuals
θ (degrees)
d)
TS (dB re 1m2)
Dorsal model
Depth (m)